Available online at www.sciencedirect.com
SCIENCE DIRECT®
Journal of Magnetic Resonance 180 (2006) 51–57
JMR Journal of Magnetic Resonance
www.elsevier.com/locate/jmr

Analysis of RF heating and sample stability in aligned static solid-state NMR spectroscopy

Conggang Li [a,b], Yiming Mo [a,b], Jun Hu [a,b], Eduard Chekmenev [b], Changlin Tian [a,c], Fei Philip Gao [a,b], Riqiang Fu [b], Peter Gor'kov [b], William Brey [b], Timothy A. Cross [a,b,c,*]

[a] Department of Chemistry and Biochemistry, Florida State University, Tallahassee, FL 32310, USA
[b] National High Magnetic Field Laboratory, Florida State University, Tallahassee, FL 32310, USA
[c] Institute of Molecular Biophysics, Florida State University, Tallahassee, FL 32310, USA

Received 11 October 2005; revised 16 December 2005
Available online 17 February 2006

Abstract

Sample instability during solid-state NMR experiments frequently arises due to RF heating in aligned samples of hydrated lipid bilayers. A new, simple approach for estimating sample temperature is used to show that, at 9.4 T, sample heating depends mostly on ^{1}H decoupling power rather than on ^{15}N irradiation in PISEMA experiments. Such heating for different sample preparations, including lipid composition, salt concentration and hydration level was assessed and the hydration level was found to be the primary parameter correlated with sample heating. The contribution to RF heating from the dielectric loss appears to be dominant under our experimental conditions. The heat generated by a single scan was approximately calculated from the Q values of the probe, to be a 1.7 °C elevation per single pulse sequence iteration under typical sample conditions. The steady-state sample temperature during PISEMA experiments can be estimated based on the method presented here, which correlates the loss factor with the temperature rise induced by the RF heating of the sample.

Keywords: RF heating; Sample stability; Temperature measurement; Non-spinning sample; PISEMA; Solid-state NMR

1. Introduction

Radio frequency heating of biological solid-state NMR samples is a well known problem. In particular, meaningful studies of membrane proteins require the observation of well hydrated samples and often require the use of negatively charged lipids and hence counter ions. Furthermore, due to the dramatic influence of the gel to liquid crystalline phase transition, membrane protein samples are often characterized above this phase transition reflecting the native membrane protein environment and hence the need to work at temperatures above room temperature for many lipids. For solid-state NMR of aligned samples using glass slides, even with the 30 μm thick glass now available, the filling factor for the RF coil is small and therefore, relatively large samples are required and hence very high RF power levels. All of these factors have the potential to exacerbate RF heating that leads to a dangerously high temperature for these temperature sensitive samples. In addition thermal gradients across the samples lead to additional problems. Here, we demonstrate an approach for measuring the internal temperature of aligned membrane protein samples for solid-state NMR and we characterize how the samples are being heated by radio frequency irradiation. Such characterizations suggest approaches for minimizing the heating effect.

The heating of aligned membrane protein samples can have several consequences. Visually, the sample may become cloudy in the center with droplets of water forming on the interior of the glass tube containing the stack of

* Corresponding author. Fax: +1 850 644 1366.
E-mail address: cross@magnet.fsu.edu (T.A. Cross).

1090-7807/$ - see front matter © 2006 Elsevier Inc. All rights reserved.
doi:10.1016/j.jmr.2006.01.013

glass plates. In other words, the central portion of the sample has been significantly dehydrated; so that there is a hydration gradient across the sample. Via thermal or hydration gradients, the mosaic spread in bilayer alignment may significantly increase. Not only is the protein likely to be functionally and structurally sensitive to an increase in temperature, but the protein–lipid complex may also undergo a phase separation either as a result of the temperature or hydration gradient [1]. Consequently, it is of great importance to minimize the radio frequency heating of membrane protein samples.

RF heating of biological samples has been discussed by various authors [2–5] in the early literature and RF heating by solid-state NMR has been studied by many others in the more recent literature [6–19]. The sample can induce a loss in RF efficiency for generating B_1 fields by two mechanisms. Inductive losses are proportional to ion conductivity and dominate many solution NMR situations [5]. Ion conductivity can also be an important part of the dielectric loss. However, dielectric losses also derive from oscillating dipoles interacting with the oscillating electric field and therefore has a maximum effect at $\omega\tau = 1$, where ω and τ denote the RF frequency and the correlation time of the sample's dipole. Bulk water has such a critical frequency in the low to mid-GHz range ($\sim$20 GHz). For constrained water molecules interacting with a surface such as the waters in the lipid bilayer interfacial region the correlation times are reduced by 1–2 orders of magnitude and hence the critical frequency is much lower [20,21,33,34].

Recently, the importance of both ion and dielectric conductivity for solution NMR samples has been demonstrated in the reduced quality factor of cryogenic probes leading to a loss in NMR sensitivity at high fields [6,7]. Indeed, quality factors are an important characterization of all NMR probes. Here, for aligned membrane protein samples we show a quantitative correlation between the quality factor and observed RF heating.

Measurement of sample temperature for solid-state NMR has been the object of considerable literature pointing to the many reasons why it is important to know the temperature and that it is not enough to know the temperature of the gas flowing over the sample [8–13,15–17]. Thermal calibration is usually achieved by the chemical shift temperature dependence of reference compounds, such as lead nitrate, added to the sample. However, reference compounds can interact specifically with the sample. Therefore, adding a ^{207}Pb RF channel or making a channel broadband does not fulfill the need. Furthermore, since our samples are static the observation of spectral discontinuities as opposed to isotropic resonances reduces the precision of the measurements [11,16]. Recently, a fiber optic infrared temperature measurement system has been designed for MAS spectroscopy, but it is not very effective for the temperature range we are interested in [17]. Here, we will use chemical indicators within the sample tube to report on the maximum temperature achieved during the experiment.

2. Experimental

2.1. Temperature measurements

The temperature measurement method is illustrated in Fig. 1. The irreversible temperature indicator (Omega ML4C non-reversible temperature monitor, Omega Engineering (Stamford, CT)) is attached to the surface of the stack of glass slides sealed in a glass tube. The white dot above the indicated temperature value changes to black indicating the temperature has been exceeded. Two indicator strips were used in this work, one strip contains the values 40, 43, 46, and 49 °C, and the other contains 54, 60, 65, and 71 °C indicators, so the lowest and highest temperature we can measure are 40 and 71 °C, respectively. Control experiments of several types were used to show that these indicators were appropriate. First, a sample tube with only an indicator strip was tested. Under the application of an RF field, the indicator did not change color indicating that it does not directly absorb the RF energy. Second, measurements at different air flow temperatures from 40 to 72 °C were carried out in sample tubes containing only temperature indicator strips. In each case, the indicator dye turned black within 1 °C of the air flow temperature value as measured by a thermocouple. Finally, 0.5, 1, 2, 4 and 8 h PISEMA experiments were carried out on our test sample. After 1 h, no further changes in temperature were observed, so we conclude that the sample reached its steady-state temperature within this time frame under the probe conditions declared below. All further experiments were conducted for 1 h.

2.2. NMR experimental conditions

All experiments were carried out on a Bruker DRX 400 spectrometer at ^{15}N and ^{1}H Larmor frequencies of 40.596 and 400.533 MHz, respectively. A NHMFL built double resonance probe was used. PISEMA [25–27] experiments

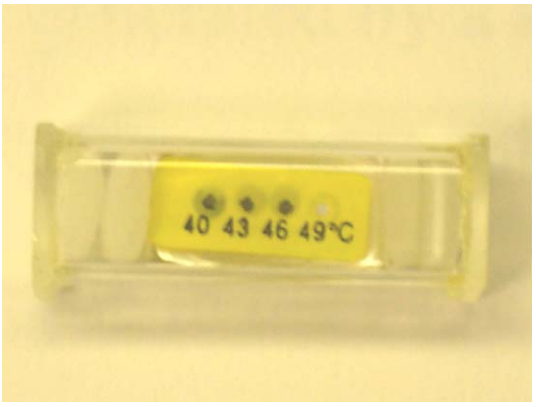

Fig. 1. Temperature measurement is based on temperature indicator strips. The strip is attached to the surface of the glass slides and sealed in the glass tube. The accuracy of the indicator is ±1 °C. Here, the strip indicated that the maximum temperature of the sample reached between 46 and 49 °C. This is reported in Table 1 as 47.5 ± 2.5 °C.

include three main parts: cross polarization (CP), spin exchange at the magic angle (SEMA) and decoupling. CP and SEMA have dual channel irradiation, while decoupling required only the ^{1}H channel. The contact time for cross polarization was 1 ms, the SEMA t_1 duration was 1.05 ms, the acquisition time was 7 ms, and the recycle delay used here was 2 s. The short recycle delay was used to accentuate the heating problem. RF fields of 45 kHz were generated in both channels during CP, while during SEMA, a 36 kHz field for the ^{1}H channel and 45 kHz field on the ^{15}N channel were utilized. The decoupling power during the acquisition was 50 kHz on the ^{1}H channel. The air flow rate was 4 L/min and an air flow temperature of 30 °C was maintained during the experiments.

2.3. Sample preparation

All prepared samples for the RF heating tests followed the protocol typically employed for the M2 membrane protein samples [22] except that protein was not used here. Ninety milligrams of 1,2-dioleoyl-*sn*-glycero-3-phosphocholine (DOPC) and 10 mg of 1, 2-dioleoyl-*sn*-glycero-3-[phospho-*rac*-(1-glycerol)] (DOPG) (Avanti, AL) dissolved in chloroform were mixed together and vacuum dried overnight. Ten percent octylglucoside (OG) was used to dissolve the dried mixture until the solution became transparent. The 8 ml solution was then dialyzed against 2 L of water or phosphorous buffer and changed three times at intervals of 6 h. The lipid bilayer vesicles were pelletted by ultracentrifugation at 55,000 rpm for 4 h in a 70 Ti rotor (Beckmann Instruments, Fullerton, CA). The pellet was transferred to a small centrifuge tube. HPLC grade water was added to re-suspend the pellets to a final volume of 3 ml. Aliquots were spread on 33 glass slides ($12 \times 5.7 \times 0.07$ mm). The sample was dried and then incubated at the desired relative humidity controlled by different saturated salt solutions [24], i.e, 32% ($CaCl_2$), 67% ($CuCl_2$), 86% (KCl), 97% (K_2SO_4), and 98% (Na_2HPO_4) for several days until equilibrium was reached. The glass-plates were subsequently stacked and inserted into the sample tube with a temperature indicator strip in the humidity chamber before sealing the sample prior to the NMR experiment.

2.4. Measurement of the RF loss factor

The loss factor $\mathrm{LF} = (Q_U - Q_L)/Q_U$, corresponds to the fraction of the applied RF power that heats the sample. It was determined by measuring Q values of the probe with (Q_L) and without (Q_U) the sample. The Q values were measured using a HP network analyzer. It is simple to show that the loss factor can be converted into an effective series resistance (ESR) of the sample using the relationship $\mathrm{ESR} = \omega L \cdot \mathrm{LF}/Q_L$ (where ω is the resonant frequency and L is the inductance of the coil). The coil contains 4.25 turns of AWG 14 copper wire with a mean diameter of 11.5 mm and a length of 9 mm. Its inductance as calculated by standard means is 150 nH. For the experiments described here, ωL is a constant and equal to 120π, so that $\mathrm{ESR} = 120\pi \cdot \mathrm{LF}/Q_L$. The solenoid coil and the RF probe were the same as those employed for temperature measurements of the lipid bilayer samples.

3. Results and discussion

Temperature and ^{1}H loss factor measurements were made for samples having a range of hydration level and salt concentration prepared as described in Section 2.3. Temperature measurements were made after 1 h of the PISEMA experiment described in Section 2.2. The results are listed in Table 1 and indicate that over the range of hydration level (0–98%, relative humidity) and salt concentration (0–80 mM) tested, power absorption and resulting sample temperature increase monotonically with both hydration and salt concentration.

Tests (Fig. 2A) were made to determine whether the ^{15}N or ^{1}H field produced a larger heating effect. The sample tested contained DOPC/DOPG (9:1 weight ratio) dialyzed

Table 1
Loss factor and steady-state temperature of different samples with an air flow temperature of 30 °C

Sample condition No.	Lipid composition (total 100 mg, dry weight)	Phosphate salt concentration in the dialysis buffer (mM)	Hydration level, relative humidity (%)	^{1}H loss factor	Steady-state temperature (°C)[a]
1	Control (only glass-slides and water)	0	100	0.01	35 ± 6
2	DOPC	0	32	0.06	35 ± 6
3	DOPC	0	67	0.13	44.5 ± 2.5
4	DOPC	0	97	0.18	57 ± 4
5	DOPC/DOPG = 9:1	5	0	0.03	35 ± 6
6	DOPC/DOPG = 9:1	5	67	0.12	47.5 ± 2.5
7	DOPC/DOPG = 9:1	5	86	0.17	51.5 ± 3.5
8	DOPC/DOPG = 9:1	5	98	0.22	57 ± 4
9	DOPC/DOPG = 9:1	5	97	0.19	57 ± 4
10	DOPC/DOPG = 9:1	10	97	0.22	57 ± 4
11	DOPC/DOPG = 9:1	20	97	0.24	57 ± 4
12	DOPC/DOPG = 9:1	40	97	0.26	62.5 ± 3.5
13	DOPC/DOPG = 9:1	80	97	0.29	68 ± 4

[a] For each sample, two temperature indicator strips (40/43/46/49 and 54/60/65/71) were used to measure the steady-state temperature.

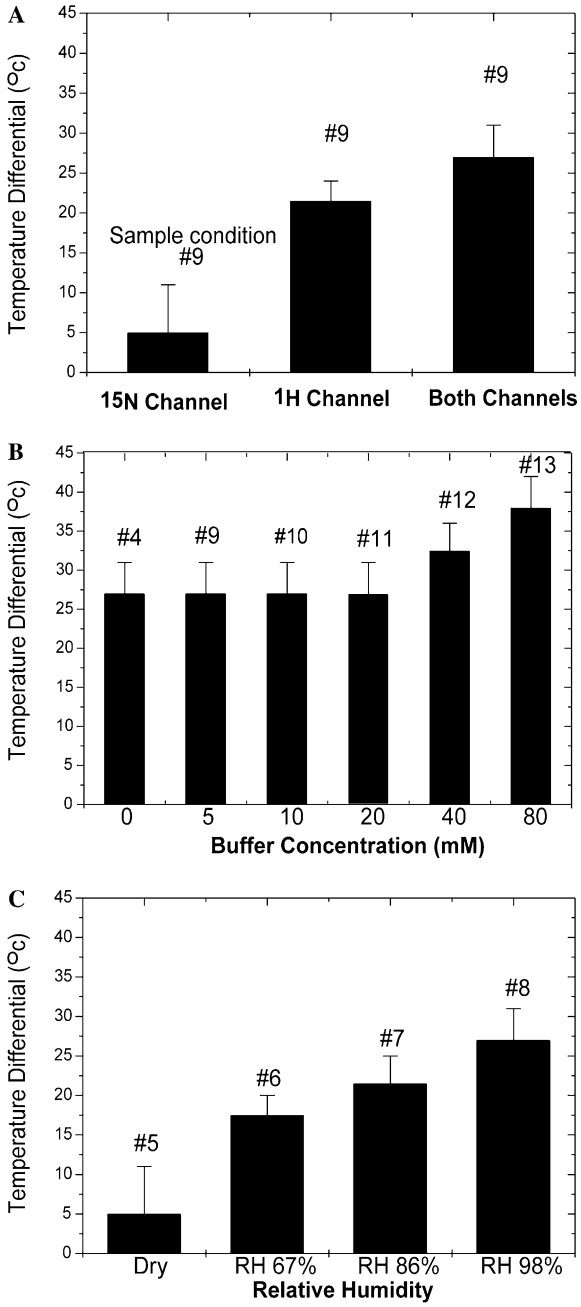

Fig. 2. Experimental conditions used for these experiments are: CP contact time, 1 ms; ^{1}H and ^{15}N B_1 fields, 45 kHz; acquisition time, 7 ms; decoupling B_1 field 50 kHz; recycle delay, 2 s; the SEMA t1 domain, 1.05 ms; air flow rate, ~4 L/min at 30 °C. The sample is DOPC/DOPG in a 9:1 weight ratio with approximately 3.3 mg/slide and 33 slides. Sample numbers are labeled on the top of each histogram column and the sample conditions are listed in Table 1. (A) RF frequency effect on sample heating; ^{15}N channel operational only, ^{1}H channel operational only, both channels operational. (B) Influence of salt concentration in the dialysis buffer on sample heating. (C) Influence of hydration level on sample heating.

in 5 mM phosphate buffer and rehydrated at 97% relative humidity. When only ^{15}N irradiation is used, no temperature change was observed from the indicators (the lowest indicator is 40 °C requiring a 10 °C temperature rise to trigger the sensors and consequently the temperature increase is reported as 5 ± 6 °C). The 49 °C indicator was triggered with ^{1}H pulses and is reported in Fig. 2A as a 21.5 ± 3.5 °C increase over 30 °C. An additional increase of 5 °C over that for only the ^{1}H irradiation was demonstrated when both frequencies were used, illustrating that most, but not all, of the heat was deposited by the ^{1}H channel. Because this effect was observed during a PISEMA experiment in which both the B_1 field and the duty cycle of the ^{15}N and ^{1}H channels differ, we do not propose to generalize the results of these frequency dependent measurements. However, the result may be at least in part due to the strong dependence on the frequency of the RF power absorption noted in previous work [2,3,29].

Fig. 2B shows the influence of salt concentration and lipid composition on sample heating while irradiating with both ^{1}H and ^{15}N frequencies for samples hydrated with 97% relative humidity. The first sample is only DOPC without any added buffer (salt) in the dialysis solution. The 54 °C indicator was triggered even under these minimal salt conditions and reported as 27 ± 4 °C. The other samples have both DOPC and DOPG (9:1 weight ratio) lipids present with different phosphate buffer concentrations used during dialysis. The presence of negatively charged DOPG requires counter ions and therefore, leads to a higher salt concentration in the sample, and potentially higher sample temperature. The temperature increase upon addition of DOPG was not significant compared to DOPC alone. Indeed, only when the dialysis buffer concentration was above 20 mM, was there a significant temperature increase above that observed with DOPC alone. This phenomenon demonstrates that the effective conductivity of the sample is dominated by the hydrated lipid, rather than by the salt in the lipid bilayer preparation. The contribution to the conductivity arising from salt is comparable to that of the hydrated lipid only in the presence of high salt concentration. This is not surprising because the conductivity of the salt is determined not only by its concentration, but also by its mobility and in the lipid bilayer environment the ion mobility is restricted through interactions with the lipids in the interfacial region of the lipid bilayer. The ion conductivity in such a sample may decrease by 1000-fold compared to a bulk solution of similar ion concentration [6].

Fig 2C shows the temperature dependence as a function of the relative humidity used during rehydration of the sample. The vacuum dried sample shows no temperature rise based on the indicators, the sample rehydrated at a relative humidity 67% shows a rise of 17.5 ± 2.5 °C. The temperature of a sample rehydrated at a relative humidity of 86% is elevated by 21.5 ± 3.5 °C and the temperature of a sample rehydrated at 98% rises by 27 ± 4 °C. All samples contained 100 mg DOPC/DOPG (9:1 weight ratio) and 5 mM phosphate dialysis buffer was used. Thus, the degree of RF heating is very sensitive to the level of sample hydration. According to Jendrasiak and Smith [28], all of the phospholipids exhibit a very rapid logarithmic rise in electric conductivity as the first few water molecules are

absorbed. The conductivity continues to rise with further hydration, but at a significantly slower rate. A plateau region is attained at about 20 water molecules per lipid. The hydration level achieved as a function of relative humidity is documented [31,32,34] for some lipid preparations. For example, in pure POPC membranes, it has been shown that the water molecules per lipid as a function of relative humidity is: 3.7 ± 0.3 at 44% r.h. (relative humidity), 4.2 ± 1.5 at 57% r.h., 7.0 ± 2.9 at 75% r.h., 9.0 ± 2.1 at 84% r.h., 11.4 ± 1.8 at 93% r.h. [32]. For DOPC/DOPG this correlation is not known quantitatively, but it should not be much different and hence we report only the relative humidity.

Inductive and dielectric losses are two mechanisms by which the sample can induce a loss of efficiency in generating a B_1 field and in detecting signals. Inductive losses are caused by eddy currents induced in weakly conducting samples resulting from an alternating B_1 field. This loss, also termed as eddy current loss, is induced by a nonconservative field that cannot be removed. These losses, however, can be calculated. For a solenoidal coil of radius a, length $2g$ and n ($n \geqslant 1$) turns loaded with a cylindrical sample of length $2g$ and radius b, Hoult and Lauterbur [3] showed that the power dissipation can be expressed as an effective resistance R_m

$$R_m = \frac{\pi\omega_0^2\mu_0^2 n^2 b^4 g\sigma}{16(a^2+g^2)}, \quad (1)$$

where ω_0 is the resonant frequency and σ is the ion conductivity of the sample. Therefore, for a given coil geometry and frequency $R_m \propto \sigma$ and hence the inductive loss is proportional to the ion conductivity of the sample.

The dielectric loss results from the charge distribution on the coil windings and can be identified with the distributed capacitance along the RF coil. The dielectric loss, induced by a conservative field, can be removed without jeopardizing the NMR experiment. Gadian and Robinson [2] pointed out that the maximum dielectric loss occurs when $\sigma = \omega_0\varepsilon\varepsilon_0(c_1+c_2)/c_2$, where ε is the dielectric constant of the sample, c_1 is the capacitance from sample to coil, and c_2 is the capacitance of the sample. Because it is difficult to measure the values of c_1 and c_2, the dielectric losses are far more difficult to predict. However, Gadian and Robinson [2] proposed that the losses can be experimentally determined by plotting the observed losses as a function of sample conductivity. The inductive loss is proportional to ion conductivity and the remaining loss corresponds to the dielectric loss (Fig. 3). The effective series resistance (ESR) was calculated from the measured LF as a function of sodium chloride concentration in aqueous solution ranging from 8 to 760 mM in the same size sample container as the aligned samples. At low sodium chloride concentrations, the ESR dramatically increases with concentration and at higher concentration, it somewhat decreases. The line in Fig. 3 proportional to NaCl concentration illustrates the maximum inductive loss. The difference between the experimental data and the line

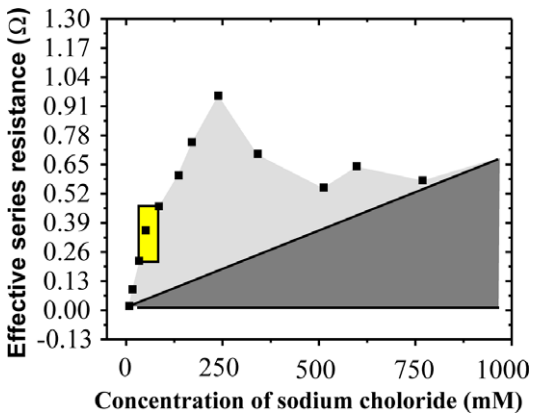

Fig. 3. Calculated effective series resistance (ESR) as a function of NaCl concentration. The Q values were measured three times using an HP network analyzer and the average value of ESR is plotted. The boxed area in the figure indicates the range of ESR and ion conductance for a typical oriented membrane protein sample. The predicted maximum inductive loss is proportional to the ion conductivity of the sample and is represented here as the boundary between the dark shaded area (inductive losses) and light shaded area (dielectric losses). Clearly, for a typical membrane protein sample the losses are dominated by dielectric losses.

representing the inductive loss corresponds to dielectric losses. It suggests that at low salt concentration (below 500 mM), the dielectric loss is very significant and it is dominant below 250 mM.

Fig. 3 has shown the experimental correlation between ESR and NaCl concentration, the latter being proportional to ion conductivity in simple solution. Fig. 4 illustrates the experimental linear correlation between loss factor and RF heating. Despite the lack of precision in the thermal indicators the data fits remarkably well to a linear solution. Our typical bilayer preparations have a loss factor between 0.17 and 0.24 corresponding to a predicted heating range from 21 to 31 °C under the experimental conditions, which have been chosen here to accentuate sample heating. Further-

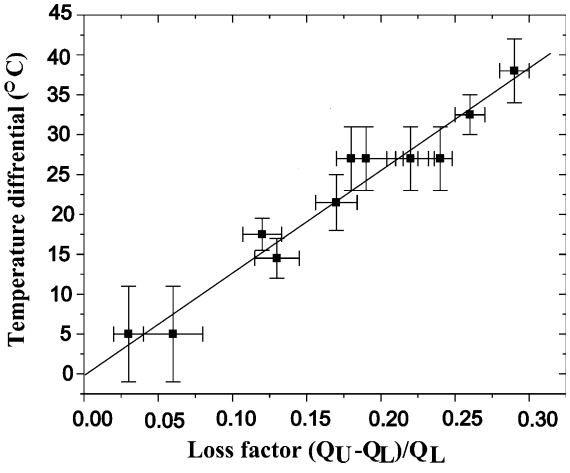

Fig. 4. Temperature rise in the sample as a function of loss factor for the samples described in Table 1. The Y axis error bar originates from the temperature measurement as described in the text. The X axis error bar is within 0.02.

more, the maximum temperature can clearly be predicted by measuring the loss factor and using this curve.

The heat deposition from a single transient (8 ms irradiation) can be estimated from the loss factor based on assuming that the power absorbed by the sample P_s, is equal to the total input power, $P = 400$ W, multiplied by the LF = 0.22, for instance. For this calculation only the ^{1}H irradiation was considered. Since there is no significant heat transport in the short 8 ms ^{1}H pulse, the total amount of energy absorbed by the sample will be $400 \times 0.22 \times 0.008 = 0.70$ J. For a 120 mg sample having a heat capacity of 3.5 J/g °C, the $\Delta t = 1.7$ °C. The observed 27 °C rise in temperature (Table 1) is therefore, the result of multiple transients for which the heat is not effectively dissipated from the sample during the 2 s recycle delay. In data not shown it has been confirmed that the maximum temperature is achieved only after 30–60 min of pulsing.

The efficient 400 MHz RF heating observed here, appears to arise from the dielectric properties of water interacting in the interfacial region of the lipid bilayer. Alper et al. [30] have predicted that the correlation time for the interfacial water is about 10 times shorter than that of bulk water through molecular dynamics simulations of dimyristoyl phosphatidylcholine (DMPC) monolayers. Recently, ultrafast time-resolved fluorescence studies indicate well-ordered interfacial water structures in reverse micelles and in cubic phase lipid [20,21]. The correlation time of the bound water in the interfacial region of lipid bilayers is about 100 times slower than bulk water [20,21]. Even for samples that are extensively hydrated, the thickness of the aqueous interbilayer band will result in a reduced averaged correlation time for the water molecules. Apparently, these samples absorb RF power very efficiently, even at 400 MHz.

Deceasing the hydration level is clearly an option for reducing RF heating as described by Marassi and Crowell [23], but in our hands, it has been difficult to reproducibly prepare well aligned samples at such low hydration levels. As a result of the RF loss being dominated by dielectric losses for our samples it will be possible to shield the sample from these losses and to minimize RF heating. Faraday shields have been shown to be effective for screening the electric fields that induce dielectric losses [2] and clearly represents an option to pursue. Moreover, considerable work on minimizing the electric fields generated by NMR probes in the sample volume, such as the scroll coil designed for magic angle spinning [14] or single turn coils (loop-gap resonator) represent an even more promising avenue for further work [35,36]. The scroll coil design takes advantage of the minimal conservative electric field generated by the scroll resonator, resulting in minimal dielectric loss [15].

4. Conclusion

Our experiments show that sample heating induced by the RF under native-like sample conditions for membrane proteins can be very substantial and largely the result of dielectric losses. These losses result mainly from significant water content and not from modest ion concentrations. Even the inclusion of a charged lipid requiring counter ions did not significantly increase the RF losses. This situation is quite different from the situation in solution NMR where even at high fields and modest salt concentrations, the RF losses are dominated by inductive losses [6]. Protection from RF heating is important not only because membrane protein samples are very sensitive to high temperatures, but also the PISEMA spectral resonance line widths are highly sensitive to changes in conformation, dynamics and orientation of the protein with respect to the magnetic field. A variation in temperature across the sample can influence all three of these factors thereby resulting in substantial line broadening. Here, we have demonstrated an understanding of heating in such samples and suggest mechanisms for minimizing the heat deposition.

Acknowledgments

The authors thank Prof. Zilm for insightful discussions. This work has been supported by DMB 0235774 from the National Science Foundation to TAC and RF and by GM-64676 from the National Institutes of Health. The spectroscopy was performed at the NHMFL supported by NSF through cooperative agreement DMR-0084173 and by the State of Florida.

References

[1] J.M. Seddon, Structure of the inverted hexagonal (H_{II}) phase non-lamellar transition of lipids, Biochim. Biophys. Acta 1031 (1990) 1–69.
[2] D.G. Gadian, F.N.H. Robinson, Radiofrequency losses in NMR experiments on electrically conducting samples, J. Magn. Reson. 34 (1979) 449–455.
[3] D.I. Hoult, P.C. Lauterbur, The sensitivity of the zeugmatographic experiment involving human samples, J. Magn. Reson. 34 (1979) 425–433.
[4] D.I. Hoult, R.E. Richards, The signal-to noise ratio of the nuclear magnetic resonance experiment, J. Magn. Reson. 24 (1976) 71–85.
[5] J.J. Led, S.B. Petersen, Heating effects in carbon-13 NMR spectroscopy on aqueous solutions caused by proton noise decoupling at high frequencies, J. Magn. Reson. 32 (1978) 1–17.
[6] A.E. Kelly, H.D. Ou, R. Withers, V. Dötsch, Low-conductivity buffers for high-sensitivity NMR measurements, J. Am. Chem. Soc. 124 (2004) 12013–12019.
[7] T. Horiuchi, M. Takahashi, J. Kikuchi, S. Yokoyama, H. Maeda, Effect of dielectric properties of solvents on the quality factor for a beyond 900 MHz cryogenic probe model, J. Magn. Reson. 174 (2005) 34–42.
[8] Bielecki, D.P. Burum, Temperature dependence of ^{207}Pb MAS spectra of solid lead nitrate. An accurate, sensitive thermometer for variable temperature MAS, J. Magn. Reson. A 116 (1995) 215–220.
[9] G. Neue, C. Dybowski, Determining temperature in a magic-angle spinning probe using the temperature dependence of the isotropic chemical shift of lead nitrate, Solid State Nucl. Magn. Reson. 7 (1997) 333–336.
[10] T. Mildner, H. Ernst, D. Freude, ^{207}Pb NMR detection of spinning-induced temperature gradients in MAS rotors, Solid State Nucl. Magn. Reson. 5 (1995) 269–271.

[11] G. Neue, C. Dybowski, M.L. Smith, M.A. Hepp, D.L. Perry, Determination of ^{207}Pb chemical shift tensors from precise powder lineshape analysis, Solid State Nucl. Magn. Reson. 6 (1996) 241–250.
[12] B. Langer, I. Schnell, H.W. Spiess, A. Grimmer, Temperature calibration under ultrafast MAS conditions, J. Magn. Reson. 138 (1999) 182–186.
[13] A.N. Klymachov, N.S. Dalal, Squaric acid as an internal standard for temperature measurements in ^{13}C MAS NMR, Solid State Nucl. Magn. Reson. 7 (1996) 127–134.
[14] J.A. Stringer, C.E. Bronnimann, C.G. Mullen, D.H. Zhou, S.A. Stellfox, Y. Li, E.H. Williams, C.M. Rienstra, Reduction of RF-induced sample heating with a scroll coil resonator structure for solid-state NMR probes, J. Magn. Reson. 173 (2005) 40–48.
[15] S.V. Dvinskikh, V. Castro, D. Sandström, Heating caused by radio-frequency irradiation and sample rotation in ^{13}C magic angle spinning NMR studies of lipid membranes, Magn. Reson. Chem. 42 (2004) 875–881.
[16] P.A. Beckmann, C. Dybowski, A thermometer for nonspinning solid-state NMR spectroscopy, J. Magn. Reson. 146 (2000) 379–380.
[17] R.W. Martin, K.W. Zilm, Variable temperature system using vortex tube cooling and fiber optic temperature measurement for low temperature magic angle spinning NMR, J. Magn. Reson. 168 (2004) 202–209.
[18] R.R. Ketchem, W. Hu, T.A. Cross, High-resolution conformation of gramicidin A in a lipid bilayer by solid-state NMR, Science 261 (1993) 1457–1460.
[19] S.J. Opella, C. Ma, F.M. Marassi, NMR of membrane associated peptides and proteins, Methods Enzymol. 339 (2001) 285–313.
[20] D.M. Willard, R.E. Roter, N.E. Levinger, Dynamics of polar salvation in Lecithin/water/cyclohexane reverse micelles, J. Am. Chem. Soc. 120 (1998) 4151–4160.
[21] W. Lu, J. Kim, W. Qiu, D. Zhong, Femtosecond Studies of tryptophan salvation: correlation function and water dynamics at lipid surfaces, Chem. Phys. Lett. 388 (2004) 120–126.
[22] C.L Tian, K. Tobler, R.A. Lamb, L.H. Pinto, T.A. Cross, Expression and initial structural insights from solid-state NMR of the M2 proton channel from influenza a virus, Biochemistry 41 (2002) 11294–11300.
[23] F.M. Marassi, K.J. Crowell, Hydration-optimized orientation phospholipid bilayer samples for solid-state NMR structural studies of membrane proteins, J. Magn. Reson. 161 (2003) 64–69.
[24] F.E.M. O'Brien, The control of humidity by saturated salt solutions, J. Sci. Instr. 25 (1948) 73–76.
[25] C.H. Wu, A. Ramamoorthy, S.J. Opella, High-resolution heteronuclear dipolar solid-state NMR spectroscopy, J. Magn. Reson. A 109 (1994) 270–272.
[26] J. Wang, J. Denny, C. Tian, S. Kim, Y. Mo, F. Kovacs, Z. Song, K. Nishimura, Z. Gan, R. Fu, J.R. Quine, T.A. Cross, Imagine membrane protein helical wheels, J. Magn. Reson. 144 (2000) 162–167.
[27] F.M. Marassi, S.J. Opella, A solid-state NMR index of membrane protein helical structure and topology, J. Magn. Reson. 144 (2000) 150–155.
[28] G.L. Jendrasiak, R.L. Smith, What does lipid hydration tell us? A minireview, Cell. Biol. Mol. Lett. 5 (2000) 35–49.
[29] D.G. Hughes, J.A. Antolak, P.S. Allen, The effect of coil geometry on the RF heating of saline phantoms: application to in vivo NMR, Phys. Med. Biol. 32 (1987) 1417–1433.
[30] H.E. Alper, D. Bassolino, T.R. Stouch, Computer simulation of a phospholipids monolayer–water system: influence of long range forces on water structure and dynamics, J. Chem. Phys. 98 (1993) 9798–9807.
[31] P.K. Rogan, G. Zaccaï, Hydration in purple membrane as a function of relative humidity, J. Mol. Biol. 145 (1981) 281–284.
[32] C.M. Moraes, B. Bechinger, Peptide related alterations of membrane-associated water: deuterium solid-state NMR investigations of phosphatidylcholine membranes at different hydration levels, Magn. Reson. Chem. 42 (2004) 155–161.
[33] A. Scodinum, J.T. Fourkas, Comparison of the orientational dynamics of water confined in hydrophobic and hydrophilic nanopores, J. Phys. Chem. B 106 (2002) 10292–10295.
[34] A.S. Ulrich, A. Watts, Molecular response of the lipid headgroup to bilayer hydration monitered by ^{2}H NMR, Biophys. J. 66 (1994) 1441–1449.
[35] W. Froncisz, J.S. Hyde, The loop-gap resonator—a new microwave lumped circuit electron-spin resonance sample structure, J. Magn. Reson. 47 (3) (1982) 515–521.
[36] F.H. Larsen, P. Daugaard, H.J. Jakobsen, N.C. Nielsen, Improve RF field homogeneity in solid-state MAS NMR using a loop-gap resonator, J. Magn. Reson. A 115 (1995) 283–286.